Synthesis and electrical properties of $In_2O_3(ZnO)_m$ superlattice nanobelt*

Tang Xin-Yue(唐欣月)[a], Gao Hong(高 红)[a]†, Wu Li-Li(武立立)[b], Wen Jing(温 静)[a], Pan Si-Ming(潘思明)[a], Liu Xin(刘 欣)[a], and Zhang Xi-Tian(张喜田)[a]‡

[a] *Key Laboratory for Photonic and Electronic Bandgap Materials, Ministry of Education, School of Physics and Electronic Engineering, Harbin Normal University, Harbin* 150025, *China*

[b] *Center for Engineering Training and Basic Experimentation, Heilongjiang University of Science and Technology, Harbin* 150022, *China*

(Received 7 July 2014; revised manuscript received 18 August 2014; published online 10 December 2014)

One-dimensional (1D) $In_2O_3(ZnO)_m$ superlattice nanobelts are synthesized by a chemical vapor deposition method. The formation of the $In_2O_3(ZnO)_m$ superlattice is verified by the high-resolution transmission electron microscopy images. The typical zigzag boundaries could be clearly observed. An additional peak at 614 cm^{-1} is found in the Raman spectrum, which may correspond to the superlattice structure. The study about the electrical transport properties reveals that the $In_2O_3(ZnO)_m$ nanobelts exhibit peculiar nonlinear *I–V* characteristics even under the Ohmic contact measurement condition, which are different from the Ohmic behaviors of the In-doped ZnO nanobelts. The photoelectrical measurements show the differences in the photocurrent property between them, and their transport mechanisms are also discussed.

Keywords: $In_2O_3(ZnO)_m$, superlattice, electrical properties

PACS: 73.63.Nm, 81.05.Dz, 81.15.Gh **DOI:** 10.1088/1674-1056/24/2/027305

1. Introduction

Transparent conducting oxide materials, which have excellent performances in touch-sensitive or optoelectronic devices, have been widely studied.[1] In particular, alloys of indium zinc oxide have shown significantly enhanced electron conductivities and mobilities compared with zinc oxide. A homologous compound $In_2O_3(ZnO)_m$ (IZO) with a superlattice structure in thin film and that in bulk material could effectively be formed by ZnO doped with In up to a certain concentration.[2,3] Furthermore, due to its fascinating electronic, optical, and magnetic properties,[4,5] the synthesis of the one-dimensional (1D) semiconductor nanostructure has attracted a tremendous amount of attention in recent years. Zhang *et al.* have already synthesized IZO nanowires (NWs) with a modulated structure, analyzed the formation of such a superlattice in detail,[6] and even filled the gap in the JCPDS database.[7] Reports on photoluminescence (PL) properties, UV emission, and cathode luminescence emission[6,8,9] for these structures have also been published. Compared with NWs, nanobelts (NBs) each have a ribbon shape with a rectangular cross section and polar charges on top and bottom surfaces.[10] To superlattice structures, NWs grow along the [0001] orientation and form an axial superlattice, while the NBs grow in the $[01\bar{1}0]$ or $[11\bar{2}0]$ direction and tend to form a planar superlattice. Owing to the complexity of characterization, relevant researches on planar superlattice NBs were reported later and less. Until 2009, Li *et al.* introduced a characterization technique and identified the planar superlattice nanoribbons made of IZO,[11] and observed an additional vibration mode at 621 cm^{-1} in the Raman spectrum.[12] However, research on the electrical properties of this structure is rather rare,[3] and the photoelectrical performance of IZO superlattice NBs has not been reported yet. In the present study, IZO NBs are synthesized by the chemical vapor deposition (CVD) method. The characterization of the sample demonstrates the formation of superlattice nanostructures, and zigzag boundaries can be clearly observed, which are found for the first time in planar superlattice NBs. The photoresponse characteristic of IZO superlattice NBs is first presented, and the study of the photoelectric properties reveals the difference between IZO NBs and In-doped ZnO (ZnO:In) NBs. The different transport mechanisms in those two structures are also discussed.

2. Experimental details

The IZO NBs were synthesized by the conventional CVD method. Firstly, ZnO and In_2O_3 mixed powder in proper proportions as source materials were placed on an alumina boat, which was inserted into a horizontal tube furnace. The silicon substrates located in the downstream were coated with an Au thin film of 2 nm. The tube furnace was heated from room temperature to 1450 °C and then kept for 20 minutes

*Project supported by the National Natural Science Foundation of China (Grant No. 51172058), the Key Project of the Science Technology and Research Project of Education Bureau, Heilongjiang Province, China (Grant No. 12521z012), and the Natural Science Foundation of Heilongjiang Province for Returned Chinese Scholars, China (Grant No. LC2013C17).

†Corresponding author. E-mail: gaohong65cn@126.com

‡Corresponding author. E-mail: xtzhangzhang@hotmail.com

© 2015 Chinese Physical Society and IOP Publishing Ltd

under a pressure of 3000 Pa. High-purity nitrogen flowed in continuously at a fixed flow rate of 100 sccm. After the furnace was naturally cooled down to room temperature, a layer of white product was obtained on the substrate. The synthesized products were characterized by scanning electron microscopy (SEM) (Hitachi, S-4800, Japan). The crystal structures of the samples were determined by x-ray diffraction (XRD) (D/MAX 2600/PC, Cu Kα radiation). The microstructure and chemical composition were investigated using a high-resolution transmission electron microscope (HRTEM) (Tecnai TF20, FEI, 200 kV) equipped with an energy dispersive x-ray (EDX) spectrometer. The Raman spectra for the samples were recorded using a micro-Raman system (JY-HR800, France) at room temperature, with a laser line of 514.5 nm used as the excitation source. In order to observe the layered superlattice structure of IZO NBs in detail by HRTEM, the sample was removed away from the substrate and embedded in resin. Then the superlattice NBs were cut into slices with a glass knife on an ultra-cutter (Leica EM UC7) after being dried.

To fabricate the individual IZO NB devices, the NBs were transferred from the grown substrate to a cleaned silicon substrate with a SiO_2 layer on the upper surface. The electrodes at both ends of an individual ZnO:In NB were deposited using the microgrid template method[13] through the thermal evaporation.[14] The metal electrode consisted of Ti with a thickness of 80 nm and Au with a thickness of 100 nm.[15,16] The distance between source and drain electrodes was about 20 μm. Thereafter, the device was annealed at 450 °C for 5 minutes in a high-purity N_2 atmosphere to improve the contact between the individual NB and the electrode. The experimental results suggest that the annealing could significantly optimize the contact between NB and electrode. Finally, silver wires were connected with electrodes as guide wires. The relevant characteristics of *I*–*V* and the photoresponse were measured by a semiconductor parameter analyzer (Agilent, B1500A) at room temperature with a He–Cd laser line of 325 nm as the excitation source. Fluorescence dynamic curves were recorded by an optical spectrometer (Andor Shamrock SR-750) powered by a tunable Nd:YAG laser-pumped optical parametric oscillator laser.

3. Results and discussion

A series of samples with different doping levels are synthesized by the CVD method. The XRD pattern shown in Fig. 1 indicates the change of crystal composition with the increase of In doping concentration. The data of the concentrations came from the SEM measurements of sample substrates. As the doping level reaches and exceeds 4.98%, there appears a set of complex peaks. These peaks might relate to a superlattice structure, according to previous experience.[3,7] Besides, when the doping level reaches a definite value, the superlattice structure might be formed in order to maintain the minimum system energy. Even so, determining the formation of the superlattice still needs further characterization, and the sample of 4.98% doping concentration (the mixture of 1.0-g ZnO and 0.2-g In_2O_3 powders is used as a precursor) is chosen as a typical representative.

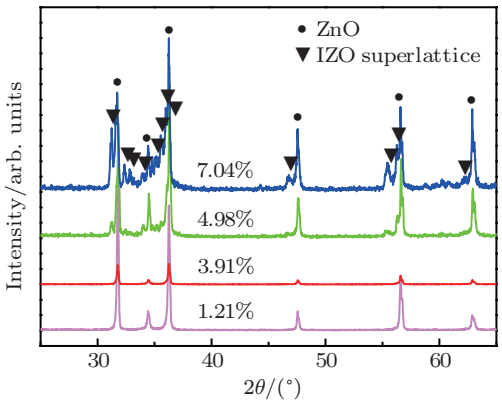


Fig. 1. (color online) XRD patterns of the samples with different In doping concentrations.

Figure 2(a) shows an SEM image of the as-synthesized products. On average, the length of the IZO NB is about tens of micrometres, and the width is hundreds of nanometers. The inset in Fig. 2(a) displays an enlarged SEM image. To obtain the detailed information about the composition of the sample, the EDX spectrum of an individual IZO NB from TEM measurement is investigated, which is shown in Fig. 2(b). The spectrometer analysis demonstrates the peaks of C, O, Zn, In, and Cu, while the signals of C and Cu are caused by the copper grid. As the IZO NBs are of planar superlattice structures, namely, the InO_2^- and $InO(ZnO)_m^+$ layers are alternately arranged along the [0001] direction,[2,17] so the cross-sectional TEM measurements are carried out. The sample is prepared by embedding NBs in the resin. Then the mixture was cut into slices with a thickness of 70 nm after being dried. Figure 2(c) shows a cross-sectional HRTEM image, which is a part of the slice cut from the individual IZO NBs. Dark and light-dark periodic bands could be clearly seen, which confirms the layered superlattice structure. The dark stripes correspond to the In–O block, and the light–dark ones are related to the In/Zn–O layer. The inset suggests the low-magnification TEM of the whole slice obtained. Figure 2(d) shows the enlarged HRTEM image of the marked area in Fig. 2(c). The image reveals a more clear layered structure and a zigzag or triangular boundary, and the angle of the zigzag shape, which is shown in the figure, is measured to be about 52°. Although a similar result has been found in superlattice nanowire,[6] it is the first time that the boundaries have been observed in a planar superlattice nanostructure. The forming of these zigzag boundaries has already been discussed.[6] In ions occupy the tetrahedral

or trigonal bipyramidal sites, which could lead to local lattice distortion. The strains are relaxed by the boundaries, which results in the crystal structure in the most stable state, thereby forming the zigzag boundaries. In addition, Yan *et al*. have proposed a zigzag modulated boundary model.[18] Because of the inversion boundaries of In–O octahedral layers, the two sides of polar ZnO are inverted. So the polarity should be inverted again in the Zn/In–O blocks, and the zigzag boundaries exist as second polarity inversions. According to the results above, the IZO layered superlattice structure is obtained.

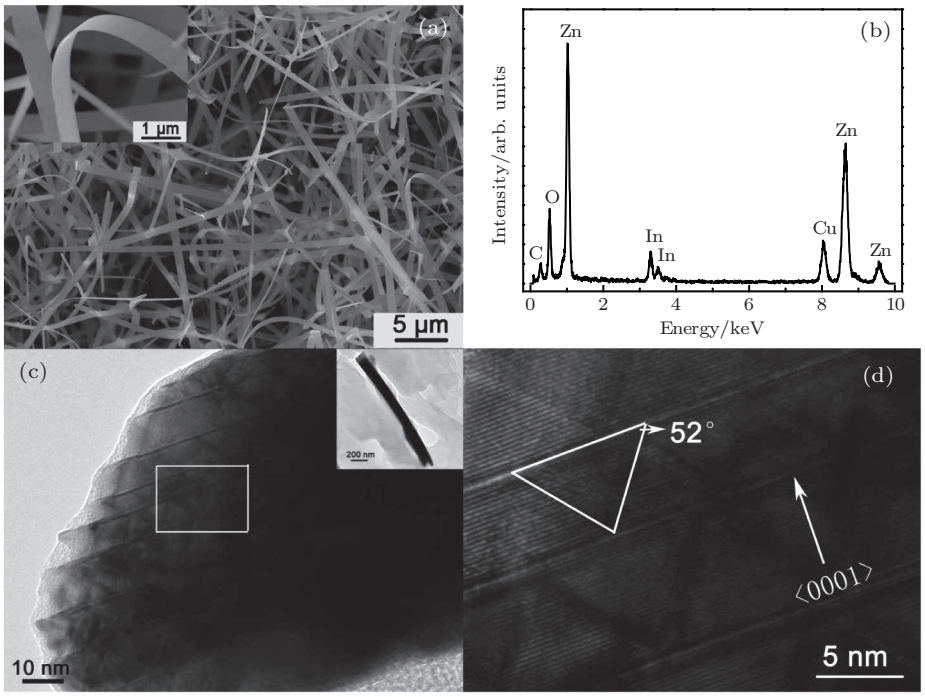


Fig. 2. (a) SEM image of IZO NBs, with an inset showing a detailed SEM image of NBs. (b) EDX spectrum of an individual IZO NB from TEM measurement. (c) HRTEM of the slice cut from an IZO NB, with an inset showing a low-magnification TEM of the whole slice. (d) Enlarged HRTEM image of the marked area in Fig. 2(c).

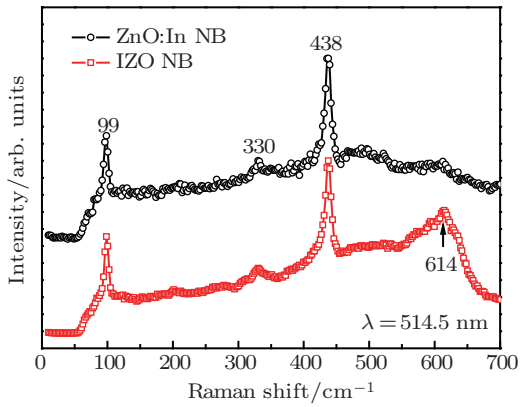


Fig. 3. (color online) Raman spectra of IZO and ZnO:In NBs.

To investigate the difference between the vibrate modes of IZO and ZnO:In NBs, the Raman spectra are measured as shown in Fig. 3. The peaks at about 99, 330, and 438 cm^{-1} correspond to the E_{2L}, E_{2H}–E_{2L}, and E_{2H} phonon modes of the ZnO, respectively. An obvious difference could be observed in the spectrum of IZO NBs, and that additional peak at 614 cm^{-1} is different from that of ZnO or In_2O_3.[19] This could be explained by the multiple-phonon scattering processes of the vibration mode, which is caused by the introduction of In ions.[20] However, it should be related to the formation of the IZO layered structure, not only the doping of In. A similar study, which attributes peaks around 621 cm^{-1} in the Raman spectrum to the superlattice, has been reported.[12]

For characterizing the electrical properties of the IZO and ZnO:In NBs, the individual NBs are used to fabricate devices. The geometric sizes of the two NBs are similar, and the two kinds of devices are fabricated using the same method. The schematic diagram is shown in Fig. 4(a). A micro-grid template method is applied to evaporating electrodes. The inset shows the functional part of the device, which is an SEM image of an individual NB between Ti/Au electrodes. The *I*–*V* properties shown in Fig. 4(b) correspond to the two types of NBs, respectively. The curves are all measured in the dark environment at room temperature. The detailed information about these two types of NBs can be observed in Fig. 4(b). Under the low applied voltage in a range approximately from −0.5 V to 0.5 V, the linear *I*–*V* characteristics for both the IZO and ZnO:In NBs indicate that the good Ohmic contacts

between the NBs and Ti/Au electrodes are achieved. The two linear curves reveal a similar transport characteristic, and also suggest that they have similar conductivities. However, the curve of IZO NBs gradually deviates from linearity when the voltage reaches a certain value, which indicates that the transport behaviors of IZO and ZnO:In NBs are significantly different. This phenomenon shows that the increase of voltage can drive the electronic transport behavior of IZO NBs from the Ohmic regime to the space charge-limited (SCL) transport regime.[21] The current shows a power law dependence on the applied voltage, i.e., $I \propto V^{\beta}$.[21] The cross-over voltage of the SCL transport regime is a function of the free carrier concentration. The smaller the carrier concentration, the lower the voltage value will be. As an intrinsic semiconductor, the carrier concentration of IZO NBs is lower than that of ZnO:In NBs. Consequently, providing a low voltage, the IZO NBs transfer to SCL but ZnO:In NBs do not. As shown in Fig. 4(b), ZnO:In NBs still follow the Ohmic behavior in the whole applied voltage range due to their high carrier concentration. These results show that the electron mobility of IZO NBs is larger than that of ZnO:In NBs. Figure 4(c) shows time-dependent photoresponse properties of the IZO and ZnO:In NBs. The data are measured at a source voltage of 1.5 V. It can be seen that in the dark environment (the duration is 0 ∼20 s), the current values are similar to those in Fig. 4(b). While under illumination (the duration is 20 s∼60 s), the photocurrents are enhanced obviously. The photo-to-dark current ratio is defined as $\eta = I_{\text{photo}}/I_{\text{dark}}$, where I_{photo} and I_{dark} are the values of the photo current and dark current, respectively. It can be obtained from Fig. 4(c) that the η of IZO NBs is 1.6, and the value of ZnO:In NBs is 2.9. That is to say, the sensitivity of the IZO NB device is lower than that of the ZnO:In. Under UV illumination, the current value of ZnO:In NBs is higher than that of IZO NBs, because the number of trapping centers in ZnO:In NBs is bigger than that in IZO NBs due to their donor doping property.[22] In the energy-providing process, the trapped electrons obtained from the excited electrons can escape from the trapping centers and participate in the transport process, then lead to a high photocurrent value for ZnO:In NBs compared with that for IZO NBs. In the recovery process (the duration is 60 s∼260 s), the current of IZO NBs decays much faster than that of ZnO:In NBs. To explore the leading factor in the recovery process, the fluorescence dynamic curves of IZO and ZnO:In NBs are recorded as shown in Fig. 4(d). The decay curves could fit to an exponential decay function[23] with a parameter τ defined as a reset time until the value recovers to $1/e$ (37%) of the maximum. The results give the relevant time constant τ of IZO NBs with a value of 251 ns, and the ZnO:In NBs with a value of 353 ns. It can be obtained that the decay time, i.e., the trapping center lifetime of IZO NBs, becomes shorter than ZnO:In NBs. In ions should act mainly as trapped electron centers in IZO NBs, but in ZnO:In NBs, the surface states play those roles. So, the difference between the two center types leads to the different lifetimes. This is consistent with the photo-generated carrier response phenomenon. Next,

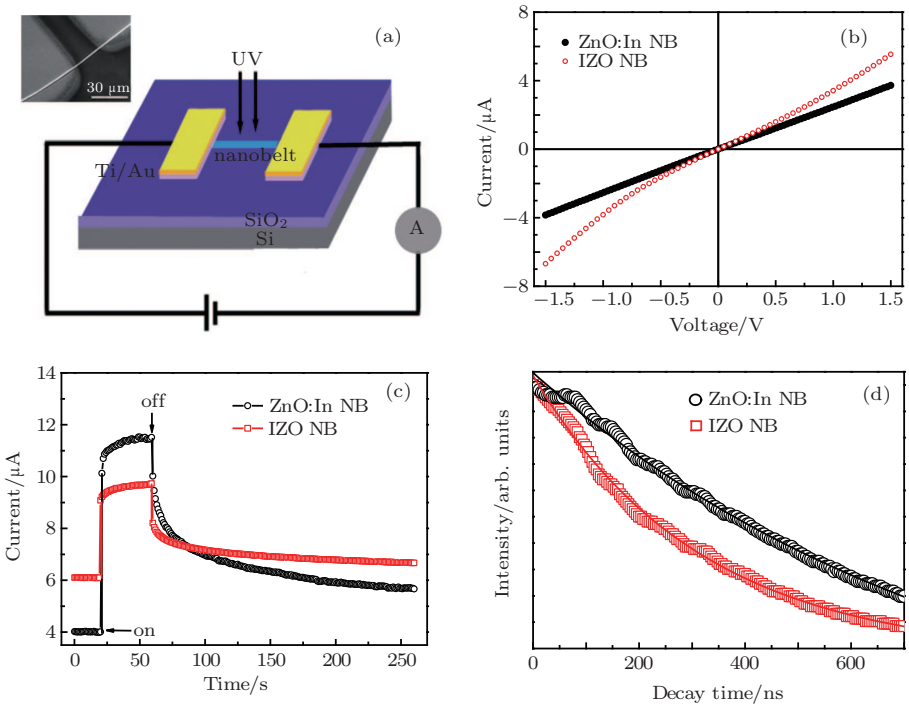


Fig. 4. (color online) (a) Schematic diagram of the individual NB device, with an inset showing an SEM image of the NB between Ti/Au electrodes. (b) Dark *I*–*V* characteristics of IZO and ZnO:In NBs at room temperature. (c) Time-dependent photoresponses of IZO NB and ZnO:In NBs at a voltage of 1.5 V. (d) Emission lifetime measurements for IZO and ZnO:In NBs.

the recovery curves shown in Fig. 4(c) fit to an exponential decay function with two time parameters, which were defined as τ_1 and τ_2. The values of the parameters for ZnO:In NBs are $\tau_{1Z} = 3.2$ s, and $\tau_{2Z} = 69$ s, while for the IZO NBs $\tau_{1I} = 0.9$ s, and $\tau_{2I} = 55$ s. Normally, the photo-recovery phenomenon could be corresponding to a faster and a slower part, which could be related to the quick combinations of electron–hole pairs and the oxygen molecules adsorption,[14] respectively. The fast recovery time τ_1 for IZO NBs is less than that of ZnO:In NBs, which is consistent with the result that the lifetime of trapped electrons in IZO NBs is shorter than that in ZnO:In NBs, as shown in Fig. 4(d). The slow recovery process is attributed mainly to the surface states and the oxygen molecule adsorption. Because the geometric sizes of the two NBs are similar, there is only a little difference in slow recovery time τ_2 between these two structures.

4. Conclusion

In this paper, IZO NBs are synthesized by the CVD method. HRTEM patterns demonstrate the formation of IZO superlattice nanostructures, and zigzag boundaries can be clearly observed, which are found in planar superlattice nanostructures for the first time. An additional peak at 614 cm^{-1} is found in Raman measurement, which may be related to the superlattice structure. The photoresponse phenomenon of IZO superlattice NBs is measured for the first time, and the results indicate that the photoelectric properties between IZO NBs and ZnO:In NBs are different. The nonlinear property of IZO NBs may be caused by the change of the transport mechanism. As an intrinsic semiconductor, the carrier concentration of IZO NBs is less than that of ZnO:In NBs, which could lead to a faster transfer to the SCL mechanism; and the number of trapping centers is also less than those of the doping materials, which may explain the difference in the photoresponse between the two NBs.

References

[1] Kim H, Lee K and Kwon J H 2006 *Appl. Phys. Lett.* **88** 012103
[2] Nomura K, Ohta H, Ueda K, Kamiya T, Hirano M and Hosono H 2003 *Science* **300** 1269
[3] Zhang J Y, Lang Y, Chu Z Q, Liu X, Wu L L and Zhang X T 2011 *CrystEngComm* **13** 3569
[4] Jie J S, Wang G Z, Han X H and Hou J G 2004 *J. Phys. Chem. B* **108** 17027
[5] Na C W, Bae S Y and Park J H 2005 *J. Phys. Chem. B* **109** 12785
[6] Zhang X T, Lu H Q, Gao H, Wang X J, Xu H Y, Li Q and Hark S K 2009 *Cryst. Growth Des.* **9** 364
[7] Niu B J, Wu L L and Zhang X T 2010 *CrystEngComm* **12** 3305
[8] Wu L L, Zhang X T, Wang Z F, Liang Y and Xu H Y 2008 *J. Phys. D: Appl. Phys.* **41** 195406
[9] Bartolomé J, Maestre D, Cremades A, Amatti M and Piqueras J 2013 *Acta Mater.* **61** 1932
[10] Wang Z L 2004 *Mater. Today* **6** 26
[11] Li D P, Wang G Z, Han X H, Jie J S and Lee S T 2009 *J. Phys. Chem. C* **113** 5417
[12] Li D P, Wang G Z and Han X H 2009 *J. Phys. D: Appl. Phys.* **42** 175308
[13] Jiang W, Gao H, Xu L L, Ma J N, Zhang E, Wei P and Lin J Q 2011 *Chin. Phys. B* **20** 037307
[14] Lang Y, Gao H, Jiang W, Xu L L and Hou H T 2012 *Sens. Actuators A* **174** 43
[15] Zhou J, Gu Y D, Hu Y F, Mai W J, Yeh P H, Bao G, Sood A S, Polla D L and Wang Z L 2009 *Appl. Phys. Lett.* **94** 191103
[16] Wan Q, Huang J, Lu A and Wang T H 2008 *Appl. Phys. Lett.* **93** 103109
[17] Alemán B, Fernández P and Piqueras J 2009 *Appl. Phys. Lett.* **95** 013111
[18] Yan Y F, Da Silva J L F, Wei S H and Al-Jassim M 2007 *Appl. Phys. Lett.* **90** 261904
[19] Berengue O M, Rodrigues A D, Dalmaschio C J, Lanfredi A J C, Leite E R and Chiquito A J C 2010 *J. Phys. D: Appl. Phys.* **43** 045401
[20] Su J, Li H F, Huang Y H, Xing X J, Zhao J and Zhang Y 2011 *Nanoscale* **3** 2182
[21] Zhao S, Salehzadeh O, Alagha S, Kavanagh K L, Watkins S P and Mi Z 2013 *Appl. Phys. Lett.* **102** 073102
[22] Keem K, Kim H, Kim G, Lee J S, Min B 2004 *Appl. Phys. Lett.* **84** 4376
[23] Ramakrishna G and Ghosh H N 2003 *Langmuir* **19** 3006